Journal of
Ship&Ocean
Technology

SOTECH Vol.2;No.1, pp. 13~30

Design of Trans-cavitating Propellers and Performance Analyses of the Test Result

Bohyun Yim, Ki-Sup Kim, Jong-Woo Ahn, Jin-Tae Lee

Korea Research Institute of Ships and Ocean Engineering(KRISO), Daeduk, Korea

Abstract

The design method for trans-cavitating propellers is considered as the combination of super- and sub- cavitating propellers. Especially the design method of the super-cavitating region of the propeller blade is elaborated. A design example is shown. Encouraging test results obtained in the Korea Research Institute of Ship and Ocean (KRISO) cavitation tunnel of a model designed by the present method are discussed.

Keywords : trans- and super-cavitating propellers, super-cavitating cascade sections, lifting line theory, lifting surface theory, experimental evaluation

1. Introduction

A trans-cavitating propeller is a combination of a super-cavitating propeller and a sub-cavitating propeller. Necessity of this type of propeller becomes clear when we recognize the advantage and the disadvantage of super-cavitating propellers. It is a well known fact that high speed propellers can not evade cavitation. That is why super-cavitating propellers were to be developed to make the efficient use of cavitation rather than evading it. However, there are many practical ships which are too slow for super-cavitating propellers, yet too fast for sub-cavitating propellers. Besides, even in fast ship propellers local relative velocities along the blades are very different according to the radial positions. That is, the relative cavitation number near the hub is too big for super-cavitation and yet that near the blade tip is too small for sub-cavitation. To fill the gap and to make safer and more efficient propellers, we need trans-cavitating propellers [Yim,1981]. The blade of this propeller is divided into two domains, one is sub-cavitating, and is denoted the domain A; and the other is super-cavitating and is called the domain B. The border line is a section line named as C(see Figure 1). The super-cavitating domain B can be either near the blade tip or next to the propeller hub according to the necessity. The former can be used for normal transitional speed ranges. The latter may be used for evading the cavitation damage near the blade root of propellers at the hub. The design program of the propeller consists of two main computer programs as usual; one is preliminary design, or lifting line design; and the other is the final design or the lifting surface design. The results of the first stage are used in the second stage. Since the problem includes both super- and sub- cavitating propellers, naturally it can treat not only trans-cavitating propellers but also pure sub-cavitating or pure super-cavitating propellers by the appropriate location of the border line C.

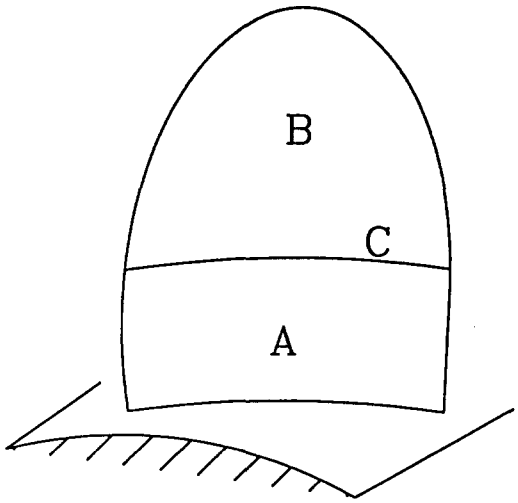

Figure 1. Trans-cavitating propeller blade

2. Preliminary design theory of trans-cavitating propellers

The preliminary design is conducted using a lifting line method. It is combined with the super-cavitating cascade theory [Yim et al, 1975, 1983] for super-cavitating sections, and the airfoil theory for sub-cavitating sections. This is to find the load distribution, the approximate blade shape and hydrodynamic pitch distribution. These results are supplied as inputs to the final design that computes final cavity, and blade shapes, and the final pitch distribution together with the thrust coefficient/power coefficient and the efficiency. In the final design a lifting surface theory is combined with an approximate method of solving an integral equation for the cavity surface.

This technique is a unique method for designing trans-cavitating propellers using a theoretical procedure without engineering guesswork. At David Taylor Model Basin (DTMB) the design theory and methods for designing super-cavitating propellers were developed for high speed ship propulsion, and several models were built and cavitation tunnel tests were conducted [Yim et al, 1983]. The results were very encouraging. The original design computer codes for super-cavitating propellers have been created and are available in DTMB. The application and improvement of the computer programs for super-cavitating propellers together with the conventional design codes for sub-cavitating propellers enable to design trans-cavitating propellers.

The theory and procedure for preliminary and final design of trans-cavitating propellers are described. The role of super-cavitating cascade model in the design process is explained to help designers select design parameters.

The extensive experimental program for trans-cavitating propellers has been conducted in the KRISO cavitation tunnel. The encouraging test results of the present design are presented in the last part of the present paper.

The super- and sub- cavitating regions are to be effectively designed in a single trans-cavitating propeller in the preliminary design stage, because both are interacting each other. The design theory for super-cavitating propellers has been developed [Yim et al, 1983] and many details can be found in the appropriate papers and reports. The theory for super-cavitating sections of trans-

cavitating propellers is exactly the same as that for super-cavitating propellers. Only difference may be the assigned cavity length near the border line C may be considerably shorter than that of a super-cavitating propeller. The section shape near the border may be hybrid such that the trailing edge shape changes gradually from the sub-cavitating region to the super-cavitating region.

The instability phenomenon of cavity length in the two dimensional super-cavitating foil for the cavity less than one and a half chord length is well known. However, whether the same phenomenon takes place in the three dimensional foil is unknown yet. There are strong doubts about it and enough evidences in numerical or experimental results that such instability may not take place in the three dimensional flow. It may be a smart decision to neglect the instability effect in the trans-cavitating propeller design and test in the tunnel. In any case, in the design of trans-cavitating propellers, it is recommendable to have distinctly separate regions where one is sub-cavitating and the other is super-cavitating with reasonably long cavity lengths, although the cavity length may be shorter or longer in the off design speeds.

Separation into two designs, the preliminary design and the final design, is convenient, as in the design of sub-cavitating propellers. In particular, the location of the basic surface where both vortex and source singularities are located is needed in the final design and obtained in the preliminary design. This, together with the lift distribution which supplies the given propeller thrust and approximate cavity source distributions are provided by the preliminary design. The final source distribution is found as the solution of the final design from the three dimensional cavity boundary conditions.

Super-cavitating sections of propeller blades have the cavity surface on the suction side, where the pressure is constant, the value of the cavity pressure. This condition imposed on the source distribution requires that a good model for super-cavitating foil sections must be used in the preliminary design. In addition, because of the strong interaction between the cavity side of a blade and the pressure side of the neighboring blade, an appropriate model is a super-cavitating cascade model [Yim, 1975, 1977].

As usual the cavitation number is defined by

$$\sigma = \frac{P_{-\infty} - P_c}{\frac{1}{2}\rho U^2} \tag{1}$$

where $P_{-\infty}$ is the pressure at far front and P_c is the cavity pressure. U is the oncoming velocity. It could be the ship speed for the cavitation number σ_s for the ship, and the local speed relative to rotating propeller blades for the local cavitation number σ_l. The cavity thickness, cavity length, the cavity drag, and the cavitation number have very close relations. Because the local radial distribution of cavitation numbers along the blade is determined according to the design speed, RPS, the propeller submergence, and the wake distribution, a special attention is needed to have low drag super-cavitating sections with a reasonable cavity thickness. Especially cavitation numbers for the trans-cavitating propellers are generally pretty large for super-cavitation near the border line C. Finding the most efficient blades for super-cavitating cascades is an important part of the preliminary design process, as discussed below.

2.1. Super-cavitating cascades

To represent mathematically the whole complicated geometry of super-cavitating blade sections of a trans-cavitating propeller, a cascade model for each section is most helpful. Each blade section

has a different hydrodynamic pitch angle β_i and blade chord length c. The distance between neighboring leading edges of propeller blades at a blade section non-dimensionalized by the chord length c is

$$d = 2\pi r/Z \tag{2}$$

where r is the radial coordinate and Z is the number of blades. This ratio of the leading edge distance to the chord length, d/c represents the solidity of the cascade at the blade section. The stagger angle is

$$\gamma = \pi/2 - \beta_i \tag{3}$$

The analyses of super-cavitating cascades are based on a well established two-dimensional coordinate transformation [Yim, 1977],

$$\begin{aligned} z &= \frac{d}{2\pi}[e^{i\gamma}\log\left\{1 - a\zeta e^{i\left(\frac{\pi}{2}-\gamma\right)}\right\} \\ &+ e^{-i\gamma}\log\left\{1 - a\zeta e^{-i\left(\frac{\pi}{2}-\gamma\right)}\right\}] \end{aligned} \tag{4}$$

$$\begin{aligned} x &= \frac{d}{2\pi}[\cos\gamma\log\left\{1 - 2a\xi\sin\gamma + a^2\xi^2\right\} \\ &+ 2\sin\gamma\tan^{-1}\left\{a\xi\cos\gamma/\left(1 - a\xi\sin\gamma\right)\right\}] \end{aligned} \tag{5}$$

$$\frac{dx}{d\xi} = \frac{d}{2\pi}2a^2\xi\cos\gamma/\left(1 - 2a\xi\sin\gamma + a^2\xi^2\right) \tag{6}$$

It is easy to recognize the reasonability of the cascade idea by comparing the two-dimensional cascades with the row of actual blade sections cut out from the propeller by a coaxial cylinder. The cascade model has been used commonly to represent a turbine blade section flow.

In the preliminary design, a lift distribution is obtained to produce a specified propeller thrust or to match a given engine power [Yim, 1994]. The lift, thrust, or engine power is closely related to the cavity drag. Thus estimation of cavity drag has to be as accurate as possible. The cavity drag is very sensitive to the cascade parameters such as solidity and stagger angle which are fuctions of blade numbers and the radial location of the section.

For designing a super- or trans-cavitating propeller a reasonable cavity thickness to accommodate a structurally adequate propeller blade is necessary. It has been often realized that a pressure distribution that produces a high lift drag ratio can result in practically meaningless negative cavity thickness [Johnson, 1958]. For a meaningful super-cavitating blade, not only the maximum thickness of the blade section but also the minimum blade thickness near the leading edge has to be considered. These thicknesses are certainly closely related to the cavity thickness. The cavity thickness along the blade is also sensitive to the cascade parameters.

There are some differences between the propeller section flow and the cascade flow. The most seemingly annoying difference is the discrepancy of cavitation numbers between a cascade and the propeller. In particular, the cavitation number of cascades with infinitely long cavities is never zero, while we know that a ventilating propeller has zero cavitation number. It is also well known that an isolated cavitating foil with an infinitely long cavity always has zero cavitation number, no matter how thick is the cavity thickness. On the other hand the cavity thickness in cascades or on propeller blades can not be too large but is limited by the solidity, or the distance between blades.

This is due to the flow continuity. Thus, the thicker the cavity, the larger the cavitation number. Of course, the cavitation number of a foil having a finite cavity is not zero under any circumstances.

In any case, an inviscid cavity flow model can not be exact but approximate. Yet it is well known that even the linear cavitating foil theory is reasonably adequate to represent an actual cavitating foil in an infinite medium. Because of the aforementioned difficulty of the cascade model, a different and a rather simpler model– a foil above the free surface in an infinite medium was suggested [Tulin, 1962]. Nevertheless, at present the author feels that the cascade model is the most reasonable model to represent super-cavitating blade sections of a trans-cavitating propeller in the preliminary design process.

A linear theory for a super-cavitating cascade has been well developed [Yim, 1977, 1975]. To design a desirable foil by the principle of superposition, three basic foils have been considered. They are, a flat plate, a low drag cambered foil such as two-term camber or five-term camber foils [Johnson, 1958],

$$\frac{y}{c} = \frac{A_1}{2}\left[\left(\frac{x}{c}\right) + \frac{8}{3}\left(\frac{x}{c}\right)^{3/2} - 4\left(\frac{x}{c}\right)^{2}\right] \tag{7}$$

$$\begin{aligned}\frac{y}{c} = \frac{A_1}{315}\Big[&210\left(\frac{x}{c}\right) - 2,240\left(\frac{x}{c}\right)^{3/2} \\ &+12,600\left(\frac{x}{c}\right)^{2} - 30,912\left(\frac{x}{c}\right)^{5/2} \\ &+35,840\left(\frac{x}{c}\right)^{3} - 15,360\left(\frac{x}{c}\right)^{7/2}\Big]\end{aligned} \tag{8}$$

where A_1 is an arbitrary constant which controls the camber and lift coefficient and a point drag [Yim.1975,1995] whose complex velocity represented by

$$w(\xi) = \frac{k_0}{K\pi i}\frac{1}{\zeta} + u_3 - iv_3 \tag{9}$$

where k_0 is the point drag strength which controls the leading edge curvature and $K = \frac{a^2 d}{2\pi}cos\,\gamma$. This supplies the cavity thickness to accommodate an adequately strong propeller blade without affecting the lift distribution and without increasing the cavity drag too much. The idea of 'point drag' is based on two-dimensional nonlinear cavity theory. The no-lift leading edge shape having the least cavity drag with a given cavity thickness at a given point is proven to be the most blunt shape, or the Kirchhoff profile K [Birkoff, 1957]. The three basic foils are superposed in an appropriate way according to the design conditions to form the blade for a super-cavitating propeller. However, the point drag model has a strong singularity at the leading edge, and the boundary condition very near the leading edge is very much violated. Although this model produces a smooth parabolic leading edge in the cavity shape [Yim, 1975],

$$\begin{aligned} y &= \bar{C}_L\left(\tan^{-1}\frac{a\xi - \sin\gamma}{\cos\gamma} + \gamma\right) / \left(2a\pi\cos\gamma\right) \\ &+ \frac{1}{\pi}\left(\frac{\sigma}{2} - u_3\right)\int_0^x \log\left|\frac{\xi - a_1}{a_3 + \xi}\right| da + v_3 x \end{aligned} \tag{10}$$

where $\bar{C}_L$ represents airfoil plane lift coefficent , the leading edge shape where the cavity separation point is located may not be too accurate. Therefore a nonlinear correction using the exact Kirchoff profile K combined with the superposed foil by matched asymptotic expansion is considered [Yim, 1995]. The pressure distribution, lift, drag, and blade cavity shape of the foil are computed.

In a rotating propeller, because of the difference in submergence, the wake distribution, and the unsteady effect caused by propeller shaft angle, the local cavitation number and the angle of attack at a given radial position changes with the rotation angle. In designing super-cavitating blade sections it is better to aim for a reasonably long cavity to prevent cavity oscillations.

In the blade, there is the transitional part from a super-cavitating section to a sub-cavitating section. If operation speeds coincide with the design speed always, the problem is not complicated. With the present design, the cavity never collapses on the blade. However, in general, the usual range of operation speeds is not very narrow. Here the cavity length may become short and collapse on the blade. Certainly, the way of collapsing may be different from that of intermittent cavitation, the isolate case without steady long cavitating region, or that of the two dimentional foil. To treat this problem, there are two methods. One is to make the super-cavitating region distinctly different so that even at the lowest allowable operation speeds the cavity length is always longer than the chord length [Yim, 1981]. In this way, there would be no danger of cavitation damage on propeller blades. However, the wider is the operation speed range, the greater the penalty in the propeller efficiency. The other method is to assume that the collapsing behavior in the trans-cavitating propeller is not too harmful, and make the blade with a gradual change from the sub-cavitating region to the super-cavitating region. Because of the three dimensional effect of trans-cavitating propellers there would not be unfavorable instability effects which occur in one and a half chord or less cavity length of two dimensional hydrofoil. More studies and experiments together with the practical experience will solve this problem.

When the lift is determined from the thrust condition, the lift and the cavitation number are the main parameters used to determine the foil shape for the super-cavitating cascade. The lift is controlled by the angle of attack and the camber shape; the cavity thickness is controlled by the point drag foil and the angle of attack. For a given cavitation number, the cavity length could be infinitely long or finite depending upon the cavity thickness. Since a larger cavity thickness causes larger cavity drag, it is always better to have a smaller cavity thickness as long as the blade strength and cavitation number conditions are satisfied.

Because a cavity length longer than two or three chord lengths behaves like a foil with an infinite cavity, it has been customary to approximate a long cavity foil as an infinite cavity foil. This fact is also true in cascades. Moreover, in cascades, because the inflow mass should be conserved between neighboring foils, the velocity is highly dependent on the cavity thickness while the cavity pressure condition indicates that the tangential velocity on the cavity must be constant. Therefore if we want to have a reasonably thick cavity to accommodate a strong thick blade at a very high speed, and if the cavity thickness is specified at a certain location along the chord, the larger the thickness, the larger the cavitation number of an infinitely long cavity. The cavitation number is sometimes larger than the design cavitation number. Often, this is the case for very high speed super-cavitating propellers. This is quite different from the case of an isolated cavitating foil where the actual cavitation number is always larger than the one approximated by an infinite cavity whose cavitation number is always zero.

For trans-cavitating propellers, local cavitation numbers are cosidered over the ranges of both

sub- and super- cavitation. The decision of the location of the border line C mostly depends upon this cavitation number distribution. To make the section in the super-cavitating region B super-cavitate with the given cavtation number, the cavity thickness or the cavity length is an only parameter to be selected. A simple decision could be to use an infinite cavity length. Then, if the given cavitation number is large, the cavity thickness becomes large, and the efficiency becomes small. Then either change the border line C near the blade tip or make the cavity length shorter. The trial and error method will reach to one of the most efficient propellers

The cavity shape along a flat plate with non-zero angle of attack behaves considerably different from that of a point drag or of the Kirchhoff profile. While the cavity shape due to a point drag is blunt near the leading edge, that of the flat plate is sharp near the leading edge; yet the latter tends to have larger trailing edge cavity thickness than the former. When the cavity thickness is specified near the leading edge, where a minimum thickness has to be maintained, the maximum blade thickness at the trailing edge varies according to the point drag strength and the blade camber. The lift of a shock-free-entry foil is totally from the basic camber, and the leading edge thickness is contributed mainly by the point drag. Thus the maximum cavity thickness along the foil may be smaller for shock-free foils than for non-shock-free-foils. i.e., the selection of the leading edge thickness is related to the amount of camber specified. However, it must be emphasized here that sizable blade camber especially near the trailing edge, as for a five-term camber foil [Johnson, 1958], is the most efficient way to maintain a high lift drag ratio to overcome the neighboring cavity interference[Tulin, 1962].

Since the design parameters such as leading edge thickness, blade shape, blade area ratio, etc. are not specified at the outset, basically a trial and error design method needs to be used. Thus we need to get some idea of how the given cavitation number is related to the cavity thickness for the case of an infinitely long cavity. Of course if the cavitation number is specified for an infinite cavity, the cavity thickness can not be specified; instead, the design computation will give the cavity thickness distribution as well as the foil shape, pitch distribution, and propeller efficiency. If the cavitation number is very small, the cavity thickness may be too small. In this case one specifies a reasonable cavity thickness distribution with an infinite cavity. Then one can not specify the cavitation number in addition. The cavitation number obtained may be larger than the design cavitation number, but the other results may be used as reasonable first approximations for the final design. The anomaly of cavitation numbers of two dimensional cascades is confined in the two dimesional space. In the final design in the three dimensional propeller flow, the design cavitation number as the three dimensional boundary conditions will correct the situation.

2.2. Vortex distributions and the basic blade pitch

Basically both preliminary and final design programs use iteration techniques. The lift, or the vortex distribution together with the pitch distribution for a sub-cavitating propeller is found by sub-cavitating propeller lifting line theory which has long been available. The differences between the sub- and super- cavitating propeller blade sections are in the cavity drag, the blade cavity geometry and the angle of attack associated with the pitch distribution. By an iteration technique, the radial vortex distribution satisfies the propeller thrust/shaft horsepower condition taking into account of the blade friction drag plus the cavity drag. The radial vortex at each propeller section is spread along the chord according to super-cavitating cascade theory [Yim, 1977], and the usual sub-cavitating propeller section theory.

Table 1. Numerical results of preliminary design

NONVISCOUS CALCULATIONS

CPT=3.9127E−01 CPS=4.6908E−01 EP=8.3412E−01
CTS=4.0337E−01 CTS/CPS=8.5991E−01

RAD	TANBI	TAN B	GS	UT/2VS
2.2000E−01	1.7251E+00	1.4702E+00	0.0000E+00	7.2417E−02
2.5000E−01	1.5302E+00	1.2938E+00	6.8866E−03	8.0513E−02
3.0000E−01	1.2867E+00	1.0782E+00	1.1553E−02	9.0095E−02
4.0000E−01	9.7350E−01	1.0862E−01	1.7578E−02	9.7886E−02
5.0000E−01	7.8062E−01	1.4690E−01	2.1351E−02	9.6283E−02
6.0000E−01	6.4984E−01	1.3908E−01	2.3330E−02	9.0201E−02
7.0000E−01	5.5529E−01	1.6207E−01	2.3576E−02	8.2390E−02
8.0000E−01	4.8374E−01	1.0431E−01	2.1838E−02	7.4228E−02
9.0000E−01	4.2768E−01	1.5939E−01	1.7173E−02	6.6348E−02
9.5000E−01	4.0397E−01	1.4047E−01	1.2739E−02	6.2607E−02
1.0000E+00	3.8258E−01	1.2345E−01	0.0000E+00	5.9025E−02

UA/2VS	DCTSI	DCPSI	CLL/D	SIGMA X
4.3213E−02	0.0000E+00	0.0000E+00	0.0000E+00	4.8017E−01
5.4026E−02	7.3738E−00	8.4594E−02	3.5371E−02	4.4064E−01
7.1656E−02	1.4964E−01	1.7322E−01	5.5021E−02	3.7960E−01
1.0248E−01	3.0984E−01	3.6183E−01	7.1834E−02	2.8049E−01
1.2535E−01	4.7934E−01	5.6108E−01	7.5363E−02	2.0996E−01
1.4067E−01	6.3798E−01	7.4598E−01	7.1914E−02	1.6067E−01
1.4994E−01	7.6080E−01	8.8685E−01	6.4213E−02	1.2586E−01
1.5064E−01	8.1234E−01	9.4276E−01	5.3129E−02	1.0077E−01
1.5095E−01	7.2339E−01	8.3503E−01	3.7684E−02	8.2273E−02
1.5062E−01	5.6791E−01	6.5362E−01	2.6634E−02	7.4826E−02
1.5074E−00	0.0000E+00	0.0000E+00	0.0000E+00	6.8324E−02

VISCOUS CALCULATIONS

CPT=3.6508E−01 CPS=5.8176E−01 EP=6.2755E−01
CTS=3.7637E−01 CTS/CPS=6.4696E−01

RAD	CL	ALFAD	P/D	DOL	DCTS
2.200E−01	0.000E+00	0.000E+00	1.192E+00	0.000E+00	0.000E+00
2.500E−01	8.362E−02	0.000E+00	1.202E+00	0.000E+00	7.081E−02
3.000E−01	1.186E−01	0.000E+00	1.213E+00	0.000E+00	1.462E−01
4.000E−01	1.433E−01	0.000E+00	1.223E+00	0.000E+00	3.055E−01
5.000E−01	1.503E−01	0.000E+00	1.226E+00	0.000E+00	4.744E−01
6.000E−01	1.510E−01	−3.761E+00	1.409E+00	1.404E−01	5.743E−01
7.000E−01	1.485E−01	−4.477E+00	1.457E+00	1.529E−01	6.906E−01
8.000E−01	1.462E−01	−4.335E+00	1.460E+00	1.407E−01	7.517E−01
9.000E−01	1.467E−01	−4.773E+00	1.499E+00	1.471E−01	6.735E−01
9.500E−01	1.545E−01	−3.890E+00	1.448E+00	1.165E−01	5.380E−01
1.000E+00	0.000E+00	0.000E+00	1.202E+00	0.000E+00	0.000E+00

DCPS	MTB	MQB	MXO	MYO
0.000E+00	9.464E+02	6.928E+02	1.074E+03	4.714E+02
8.603E−02	8.855E+02	6.444E+02	1.024E+03	3.887E+02
1.756E−01	7.850E+02	5.656E+02	9.283E+02	2.727E+02
3.671E−01	5.881E+02	4.135E+02	7.099E+02	1.139E+02
5.707E−01	4.132E+02	2.835E+02	5.001E+02	3.080E+01
9.223E−01	2.554E+02	1.671E+02	3.052E+02	−9.709E−01
1.152E+00	4.389E+02	8.761E+01	1.639E+02	−9.185E+00
1.244E+00	4.722E+01	2.788E+01	5.465E+01	−4.539E+00
1.150E+00	9.680E+00	5.462E+00	1.105E+01	−1.216E+00
8.648E−01	0.000E+00	0.000E+00	0.000E+00	0.000E+00
0.000E+00	0.000E+00	0.000E+00	0.000E+00	0.000E+00

2.3. Thrust, power and efficiency

By integration of blade lift distribution, as in the case of a sub-cavitating propeller, the normal force on the blade is obtained. Computing the induced, frictional and cavity drags, the tangential force is obtained. Thus, thrust and power coefficients and the efficiency are obtained as for a sub-cavitating propeller.

In Table 1, the results of a preliminary design for 882mm(34.72 inch) diameter and 4 bladed trans-cavitating propeller for 34 knot air cushion vehicle is presented. The submergence of the center of the propeller is at 390mm(15.36 inches). In Table 1, the results of a preliminary design for 882mm(34.72 inch) diameter and 4 bladed trans-cavitating propeller for 34 knot air cushion vehicle is presented. The submergence of the center of the propeller is at 390mm(15.36 inches). In the table, CPT is the thrust horsepower coefficient; CPS is power loading coefficient; CTS is the thrust loading coefficient. UT,UA, and VS are the induced tangentail, the induced axial and the ship speed respectively. EP represents the efficiency.

3. Final design of trans-cavitating propellers

The basic surface where both vortex and source singularities are located is needed in the final design. This, together with the approximate singularity distributions are provided by the preliminary design. In the following, the procedure of the final lifting surface design is described. The final design is conducted using a lifting surface method.

3.1. Lifting surface theory of trans-cavitating propellers

The lifting surface design in trans-cavitating propellers takes into account both super- and sub-cavitating regions in a single propeller in the same design. The design theory with the super-cavitating lifting surface has been developed [Yim et al, 1978, 1983, 1974] and many details can be found in the appropriate papers and reports. An important difference between the lifting surface theory of sub- and super- cavitating propeller blade sections is the difference in the blade and cavity thickness. Since the three dimensional cavity thickness is not known a priori, this has to be solved by an integral equation with the linear cavity surface boundary conditions. Thus only in the super-cavitating region of trans-cavitating propeller, the unknown cavity thickness has to be solved. However, the solution very much depends on the location of the border line C, the chord distribution, blade area ratio and blade thickness of the sub-cavitating region. In the present theory, to obtain the three dimensional cavity source strength, the two dimensional cascade cavity source distribution obtained in the preliminary design is multiplied by a double polynomial of both radial and chordwise coordinates with unknown coefficients, and a system of simultaneous equations for the unknown coefficients is formed with the cavity boundary conditions of velocity components [Yim, 1978],

$$\sum_{i=1}^{I}\sum_{j=1}^{J} a_{ij}A_{lm(ij)} + \sum_{p=1}^{P}\sum_{q=1}^{Q} b_{pq}A_{lm(pq)} + \sum_{k=1}^{K} a_k A_{lm(k)}$$

$$= \begin{cases} -\frac{G}{2V_s}\frac{V_l}{V} + \frac{\sigma}{2}\frac{\dot{V}_s}{V} - \frac{U_f}{V_s} \equiv \frac{U_T^m}{V_s}, \text{on the blade plane} \\ \frac{\sigma}{2}\frac{V_s}{V} - \frac{U_f}{V_s} \equiv \frac{U_T^m}{V_s}, \text{on the cavity plane} \end{cases} \tag{11}$$

where,

$A'_{lm}s$ are integrations of source distribution both radial and tangential directions at the lth colocation point, and $m(ij)$ is the index corresponding to the unknown coefficient a_{ij}.

V_l is the local flow speed relative to the blade;

V_s is the ship speed.

$V = (V_a^2 + r^2\omega^2)^{1/2}$

U_f is the tangential velocity due to the vortex distribution at all points except the point concerned.

U_T^m is the tangential velocity component due to the source distribution only.

$V_a = V_s(1 - w)$

w =wake fraction

ω =angular speed

These simultaneous equations are solved by the least squares method. Sometimes the resulting square matrix for the solution may not behave too well. Then we consider that $a_{11} = 1, a_{i,j} = 0$

with $i = 2, 3, \cdots$ is the exactly two dimensional solution. And with a certain small weight w we consider extra equations for least square equatioms

$$\begin{aligned} wa_{11} &= w \\ wa_{ii} &= 0, i = 2, 3, \cdots \end{aligned} \tag{12}$$

The solution is now always behaving well and closer to the two dimensional solution. By the error check the reasonable solutions will be confirmed.

The hub boundary condition

$$u_r = 0 \text{ on } r = r_H$$

has been also considered as in super-cavitating propeller design, but by multiplying the correction factor to the image singularities to make the boundary condition be satisfied. Including the hub boundary condition makes the pitch near the hub smaller.

Then by plotting the stream lines, or three dimensional corrections of camber and angle of attack of two dimensional sections, the cavity shape, blade shape, and the final pitch distribution for each station are obtained. The usual method will give the thrust coefficient/power coefficient and efficiency.

3.2. Final results and iterations

The careful inspection of the final results may be necessary because the present mathematical results may be not suitable for actual propellers. The many design parameters interact each other and influence the final results. It seems to be important to recognize the tendencies. For example with the given cavitation number, the distribution of cavity thickness and the blade area ratio are very sensitive to the the cavity length, the pitch and camber distributions, and the total efficiency. Too large positive or negative camber cannot be allowed.

The chord length on the sub-cavitating region may better be longer than the super-cavitating region due to the conventional basic concept. The blade area ratio sensitively influences the pitch and camber distributions. Too much camber distribution either on the sub- or super- cavitating region might induce face cavitation. By this way, sensible iterations would attain a good systematically sound trans-cavitating propeller.

In Table 2, the numerical results of final design are shown. The pitch distribution is a little rough and it seems that the more fairing is necessary. C. F represents the camber factor. The blade section shapes of the sub-cavitating region and blade cavity shapes of super-cavitating sections are shown in Figure 2.

3.3. Experimental evaluations

KRISO has conducted an experimental program in the KRISO cavitation tunnel [Lee et al, 1982, Kim et al, 1994] to evaluate the present idea of trans-cavitating propellers and the design method . A trans-cavitating propeller was designed for a 23m Air Cushion Vehicle.

The model propeller was manufactured from this design. The experimental program included measurements of propeller performance, pressure fluctuations on the neighboring ship hull, and observations of cavities.

Table 2. Numerical results of final design

TRANS-CAVITATING PROPELLER BLADE SECTION DESIGN
FOR A GIVEN BASIC CAMBER
KRISO TC 001

DIAMETER--IN	30.72	**CHORDWISE PANELS
HUB DIAM--IN	6.70	56 RADIAL S V LINES
SPEED VS--KTS	34.00	HUB IMAGE IS INCLUDED
NO. OF BLADES	4	WITH 2 DEG SPACING
REVS PER MIN	1283.88	WAKE ANGLE RATIO= 1.0

R	P/D	ALFA(DEG)	C.L.
0.25816	1.40022	8.49649	0.14935
0.35816	1.48891	10.71381	0.14555
0.45816	1.45898	10.25006	0.17841
0.55816	1.52995	11.15033	0.22935
0.65816	1.38905	7.58275	0.18897
0.75816	1.70871	12.27339	0.20925
0.85816	1.77304	12.47228	0.20603
0.95816	1.72082	11.12106	0.18162

RESULTS OF COMPUTATION OF FORCES

R/RO	CT	CP
0.2180	-0.004	0.002
0.2668	0.121	0.146
0.3157	0.204	0.244
0.4135	0.373	0.446
0.5112	0.543	0.648
0.6090	0.645	0.882
0.7067	0.671	1.159
0.8045	0.693	1.402
0.9022	0.624	1.271
0.9511	0.494	0.943
1.0000	-0.002	0.016

CT	0.383
CP	0.619
EFFY	0.618
KT	0.165
10KQ	0.445
J(VOL)	1.048

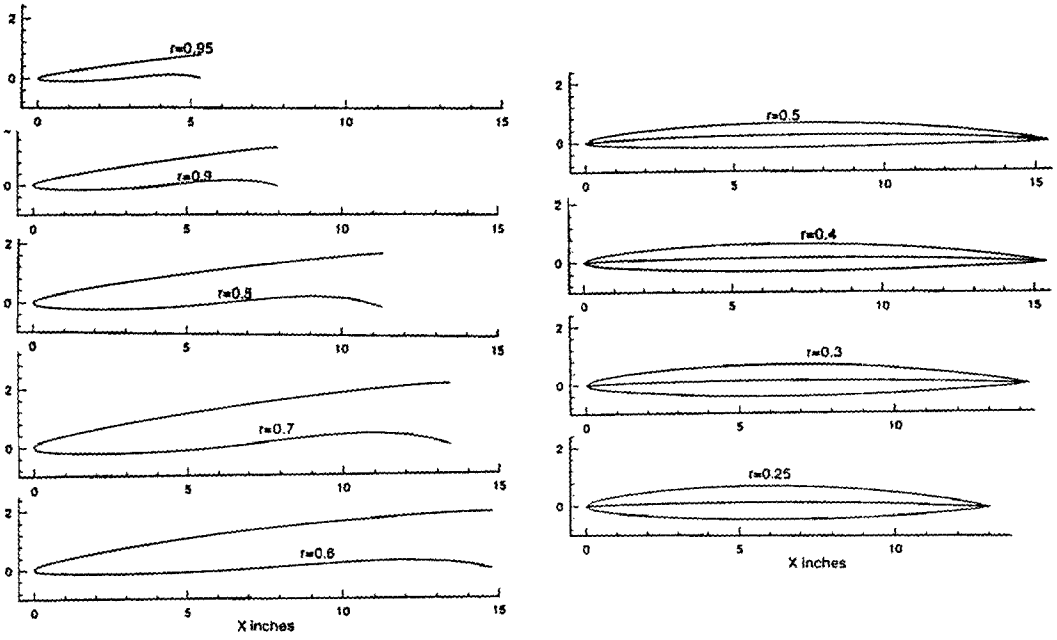

Figure 2. Trans-cavitating propeller blade sections

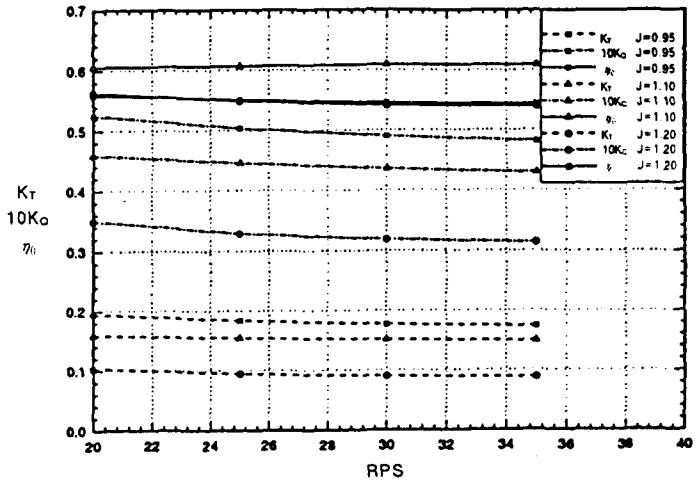

Figure 3. Viscous effect on thrust and torque at various advance coefficients ($\sigma_{s,r=0.7} = 0.65$)

3.4. Discussion of experimental results

Before measuring the propeller performance in the KRISO cavitation tunnel, to understand the viscous effects on the thrust, torque, and cavitation of the 25cm-diameter- propeller model seems necessary [Kim et al, 1991]. The measured thrust, torque and efficiency are shown in Figure 3 for the Reynolds numbers, 1.45×10^6, 1.75×10^6, 2.20×10^6 and 2.57×10^6. These are with four sets of propeller RPS's, 20, 25, 30 and 35, and a cavitation number at $r = 0.7$, $\sigma_{s,r=0.7}$=0.65 and for the various number of J values. A slight influence of the Reynolds number can be seen at lower RPS's. But at the region where RPS is more than 30, it seems to converge to a fairly even level.

In Figure 4, cavity shapes and cavitation pattern of the propeller blade are shown for various J's and RPS's, and the effects of viscous flow on cavitation pattern is found. The border line C is at $r = 0.6$. The design J is 1.048. In all cases clear separations into two regions, B, super-cavitating , and A, sub-cavitating in a single blade are seen. For higher $J > 1.2$, there exists the region of shorter cavities that are less than the chord lengths. But it looked very clean and stable in the experiments. In Figure 5 cavity shapes of propeller blades for fixed $K_T = 0.164$ and $\sigma_{s,r=0.7} = 0.65$ are shown for various RPSs. The cavity shapes do not change too much for all cases shown. This is also an encouraging information for the practical usage of trans-cavitating propellers.

According to the basic informations shown above, the performance measurements were conducted with the main dynamometer, J25 for the shaft angle zero, and with the inclined shaft dynamometer, H25 for inclined shaft mesurements [Lee et al, 1982]. These are for the fixed RPS=30 and $\sigma_{s,r=0.7} = 0.65$.

Figure 6 shows the performance curves for shaft angles, 0 degree (design value) and 12 degrees. Due to the limited tunnel dimensions, the test conditions for different shaft angles are not the same. While the model was located at the center of the tunnel for zero shaft angle, the model with shaft angle 12 degrees was placed near the bottom. This means that tunnel boundary effects

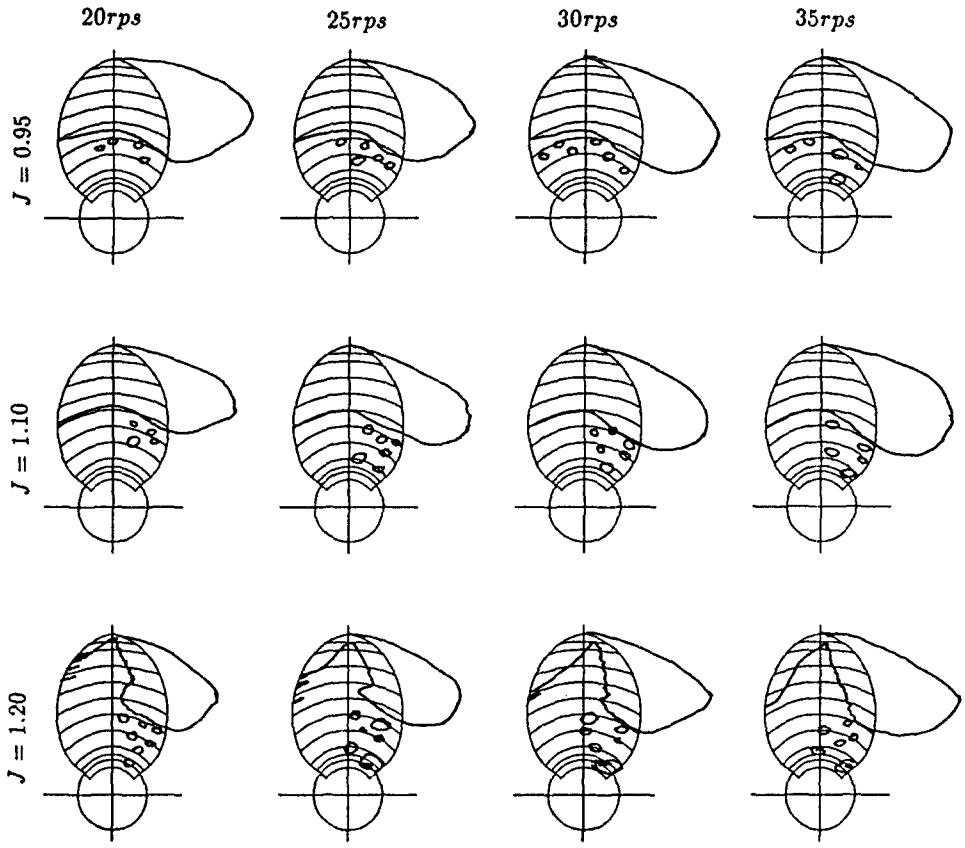

Figure 4. Viscous effect on cavitation pattern at various advace coefficient ($\sigma_{s,r=0.7} = 0.65$)

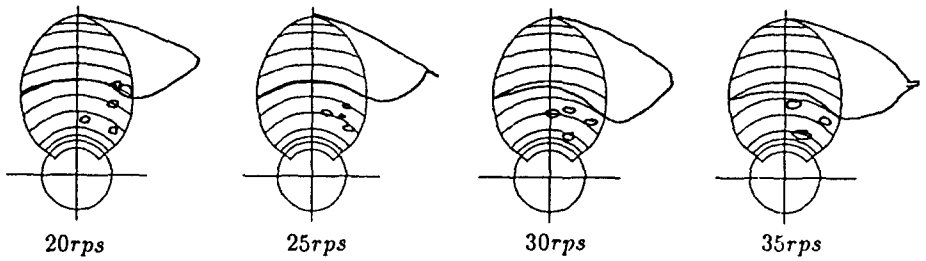

Figure 5. Viscous effect on cavitation pattern at a constant thrust coefficient ($K_T = 0.164, \sigma_{s,r=0.7} = 0.65$)

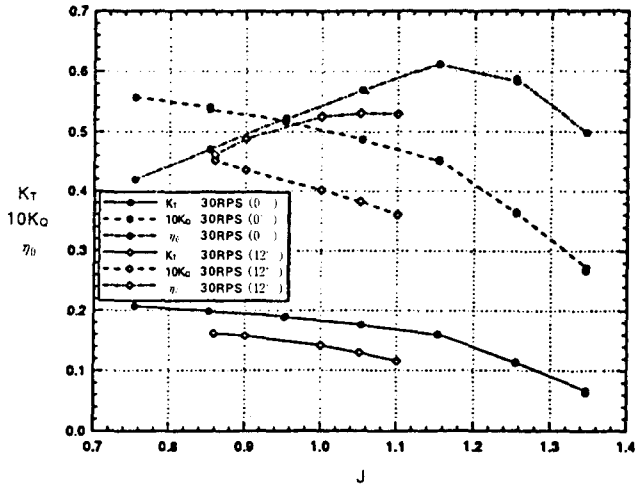

Figure 6. Characteristics of the propeller open water test on the trans-cavitating propeller with shaft angles 0^o and $12^o(\sigma_{s,r=0.7} = 0.65)$

to the test results may be different between zero and 12 degree shaft angles. Therefore the values at 12 degree shaft angle may be taken as qualitative sense. The largest efficiency is 0.62 near the design J for zero shaft angle. This is very close to the design value. Although the efficiency curve is preferable to be flat near the maximum value, the present curve shows that some improvements in design may be required.

Figure 7 shows cavity shapes for various J's at the fixed RPS and σ_s and zero shaft angle. For the large J values base cavities at the region B behind the trailing edge can always be seen due to the blunt trailing edge of the super-cavitating sections. This may be a good phenomenon [Vorus et al, 1988] because the base cavity separates smoothly at the trailing edge. Figure 8 shows cavity shapes at various rotating positions with different J's for the case of 12 degree shaft angle. In all cases no face cavity was seen and a long sheet back-cavity was seen. This is considerably different from the case of sub-cavitating propellers with the same shaft angle where a severe face cavitation is seen at the anglular position of 270 degrees. Besides, intermittent cavitations in the suction sides cause the severe propeller induced ship vibration. The less variation of cavity volume in trans-cavitating propellers is also one of the favorable features. In Figure 9, is shown a relation between the lowest radial position, r value of the sheet cavity, the corresponding J value, and the cavitation number, for zero shaft inclination.

Figure 10 shows the averaged amplitude of the pressure fluctuations versus cavitation numbers. The distance between the blade tip of the propeller and the measuring plate is 0.168D. The amplitude at the higher harmonic is observed to be much smaller than that of the first harmonic in all cases. The full scale prediction is the application of the model measurements adapted to the full scale ship for which the propeller is designed. In the design condition where border line C is located at $r = 0.6$, even the first hamonic reduces the amplitude when the cavitation number decreases, or when the cavity length increases (see Figure 11).

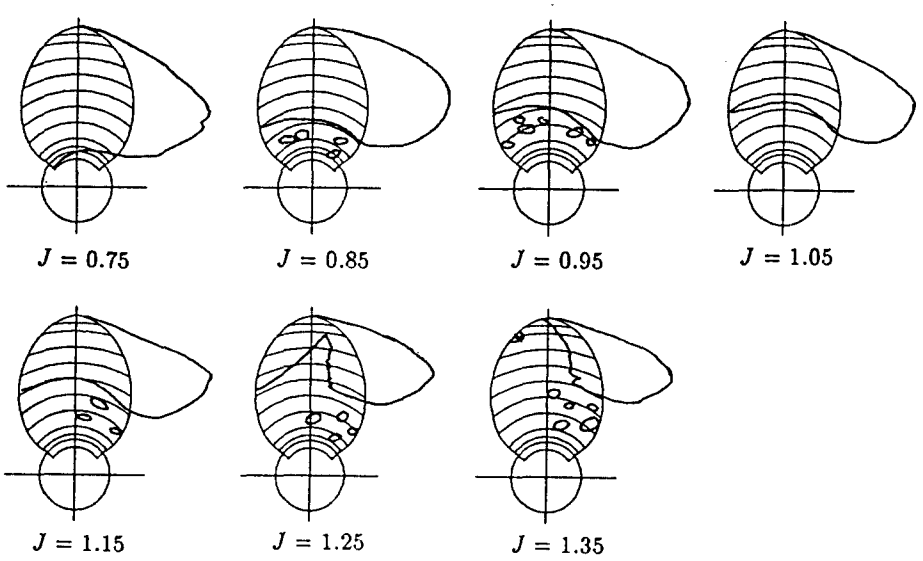

Figure 7. Sketch of cavitation pattern on the trans-cavitating propeller ($\sigma_{s,r=0.7} = 0.65$)

3.5. Conclusion

In the present design and experiments of a trans-cavitating propeller many valuable informations have been obtained. At the design conditions, the super-cavitating region and the sub-cavitating region are clearly separated without face cavitation as intended. This phenomenon stays in the reasonable neighborhood of the design conditions, that is, in the near off-design conditions. The expected efficiency has also been obtained in the design conditions. More carefull design may produce much higher efficiency, but then the beneficial operation range around the design conditions may be reduced. However, even in the range where cavity length shrinks less than the chord length, there does not seem to have the instability observed in the two dimensional foils.

The measured pressure fluctuation is small at the design cavitation number or less where the clear long cavities are present. Especially that in the higher harmonics is very small meaning that there will be no cavitation damage. Considering many other advantages of tran-scavitating propellers, this clearly indicates that trans-cavitating propellers worth serious consideration to replace the sub-cavitating propellers which have been used in spite of fluctuating cavities.

More studies are certainly necessary for the wake effects, efficiency improvement, free surface effects especially for smaller submergence, the ventilation effects, etc. The shallower submergence would be very benefical for trans-cavitating propellers because ventilation is welcomed for the super-cavitating region while it can not be allowed for sub-cavitating propellers.

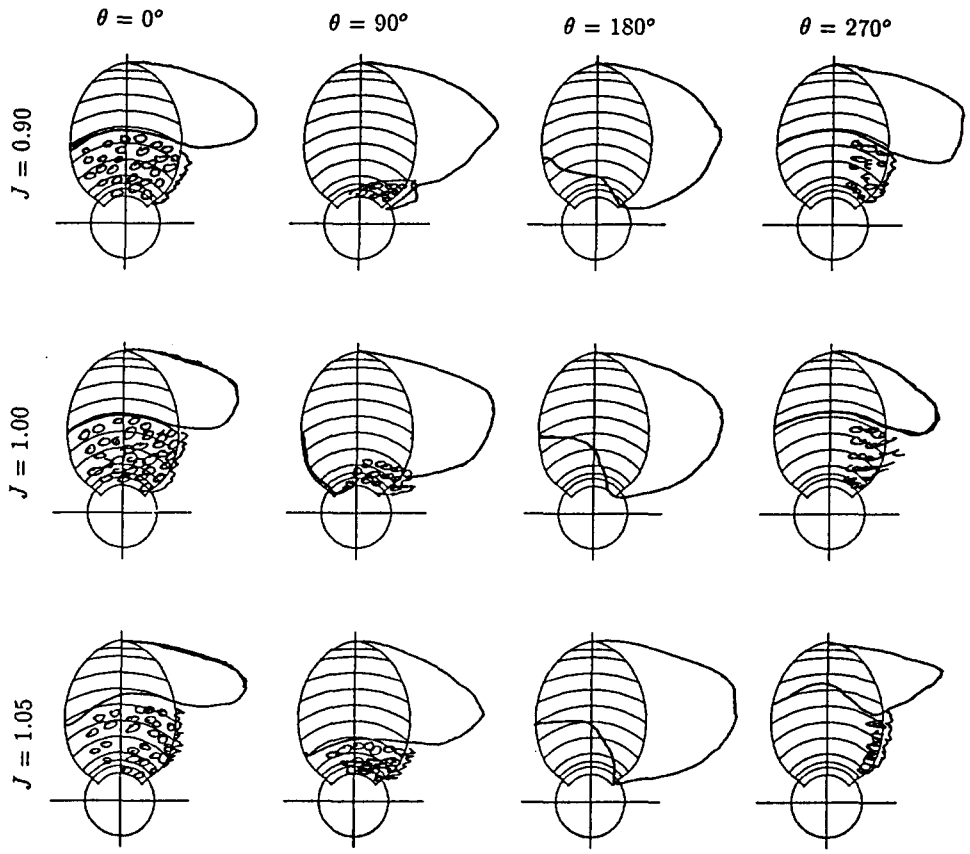

Figure 8. Sketch of cavitation pattern on the trans-cavitating propeller with an inclined shaft($\sigma_{s,r=0.7} = 0.65$)

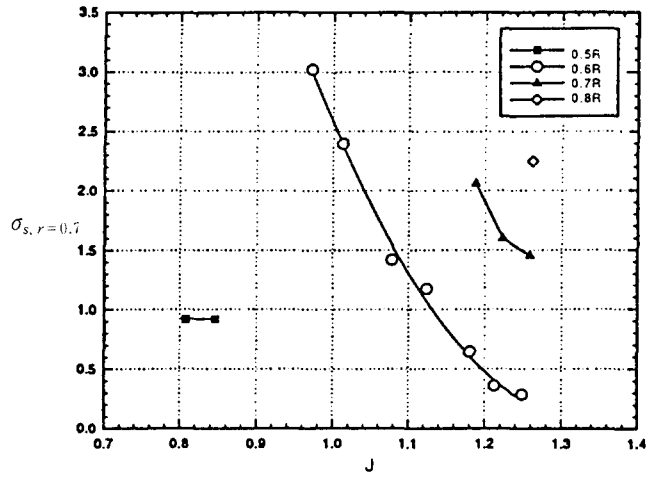

Figure 9. Cavitation inception at each blade radius

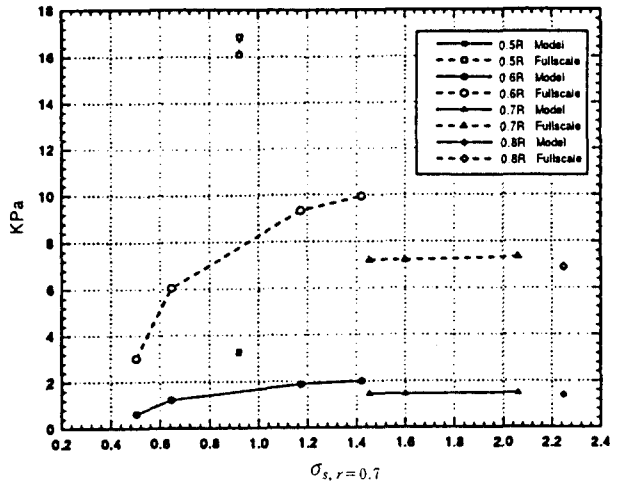

Figure 10. Measurement of pressure fluctuation at each blade radius

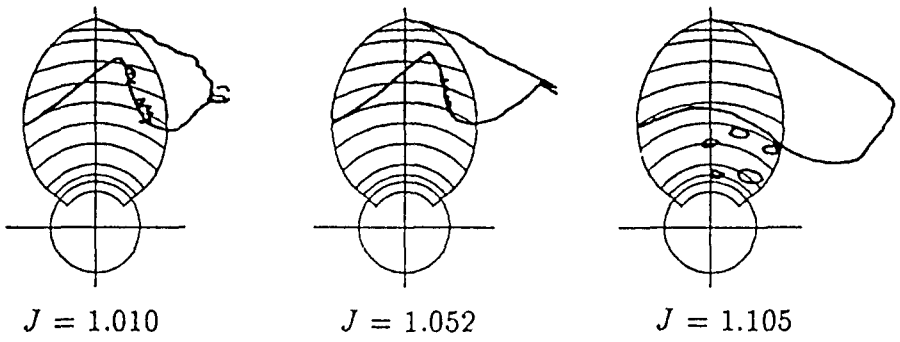

Figure 11. Sketch of cavitation at inception condition on the leading edge of radius 0.6

References

1. B. Yim, 1981(Oct.), Trans-cavitating Propellers, United States Patent Document No. 4,293, 280
2. B. Yim, 1977(Sep.), Super-cavitating Foil of an Arbitrary Shape Beneath or Above a Free Surface or in a Cascade, Proceedings of the Second International Conference on Numerical Ship Hydrodynamics
3. B. Yim, 1995, Application of Matched Asymptotic expansion for Designing a Leading Edge of Super-cavitating Section, Autumn Conference of SNAK
4. B. Yim, G. Larimer and J. Peck, 1983(Jan.), super-cavitating Propellers - Design Theory and Experimental Evaluation, DTNSRDC Report 82/068
5. B. Yim, 1994, A Preliminary Design Theory of Super-cavitating Propellers, Proceedings of Autum Meeting of the Society of Naval Architects of Korea, pp. 47-67
6. B. Yim, 1978(Jan.), A Lifting Surface Theory of super-cavitating Propellers, Proceedings of Joint Symposium on Design and Operation of Fluid Machinery Vol II, International Association of Hydraulic Research
7. B. Yim, 1975(Dec.), Finite Cavity Cascades with Low-drag Pressure Distributions, Transaction of the ASME. Vol. 97, Serioes 1, No. 4, pp. 430-438
8. V. E. Johnson, 1958, The Influence of Submergence, Aspect Ratio, and Thickness on super-cavitating Hydrofoils Operating at Zero Cavitation Number, Proceedings of the Second Office of Naval Research Symposium on Naval Hydrodynamics, pp. 317-366
9. M. P. Tulin, 1962, Super-cavitating Propeller –History, Operating Characteristics, Mechanism of Operation, Proceedings of the Fourth Office of Naval Research Symposium on Naval Hydrodynamics. ARC-92, pp. 239-286
10. G.Birkhoff and E H. Zarantonello, 1957, Jets, Wakes, and Cavities, Academic Press Inc, New York
11. W. S. Vorus, and R. F. Kress, 1988, The Sub-cavitating/Super-cavitating Hybrid Propeller, Proceedings of SNAME Spring Meating/STAR Symposium
12. C-S. Lee, K-S Kim, et al, 1982, On the Trial Operation of Cavitation Tunnel and Development of Treating Techniques, Research Report of KIMM, UCN 131 A-276.D
13. K-S Kim, K-Y Kim, J-W Ahn, and C-Y Lee, 1994, Effects of Reynolds Number, Leading Edge Roughness and Air Content on the Cavitation Performance of Model Propellers, Autumn Conference of SNAK
14. K-S Kim, K-Y Kim, J-W Ahn, and C-Y Lee, 1991, Experimental Correlation Analyses of Propeller Open-Water Characteristics at Towing Tank and Cavitation Tunnel, Autumn Conference of SNAK